EFFECT OF SOLUTION CONCENTRATIONS ON THE STRUCTURE AND PROPERTIES OF NANOFIBROUS YARNS BY BLOWN BUBBLE-SPINNING

by

Hao DOU[a], Kun-Bin KUANG[a], Yun-Yu LI[a], Wei FAN[a], Yue SHEN[b], Hong-Yan LIU[c], and Ji-Huan HE[d,e*]

[a] School of Textile Science and Engineering, Xi'an Polytechnic University, Xi'an, Shaanxi Province, China
[b] School of Science, Xi'an, Xi'an University of Architecture and Technology, Shaanxi Province, China
[c] School of Fashion Technology, Zhongyuan University of Technology, Zhengzhou, China
[d] School of Mathematics and Information Science, Henan Polytechnic University, Jiaozuo, China
[e] National Engineering Laboratory for Modern Silk, College of Textile and Engineering, Soochow University, Suzhou, China

Original scientific paper
https://doi.org/10.2298/TSCI200301101D

Solution properties play a critical role in manufacturing of nanofibrous materials. In this paper, solution concentrations were explored for the effective fabrication of nanofibrous yarns by the blown bubble-spinning. The surface tension and rheological property of spun solutions were investigated, and the product's thermal and mechanical properties were characterized.

Key words: *thermodynamic, nanofibrous yarns, solution concentrations, structure and properties, bubble spinning*

Introduction

Development of multi-levelled nanofibrous materials with advanced functions is critical for current applications such as filtration, biomedicine, sensors and smart wearable clothing. Nanofibers and nanofibrous yarns are great candidates to meet high requirements for these multi-functionalities by different assemblied and composited methods [1].

Several methods have been reported for fabrication of the yarns, such as conjugate electrospinning [2], self-bundling electrospinning [3], and water vortex electrospinning [4]. Baniasadi *et al.* [5] firstly fabricated nanofibrous PVDF-TrFE ribbons and then got yarns via twisting ribbons and finally obtained nanofibrous coils by over-twisting. However, problems still existed on the preparation of nanofibrous yarns by electrospinning, such as inefficient production, clogging needles, and electricity hazard [6, 7]. Recently, the bubble spinning, including mainly the bubble electrospinning and the blown bubble-spinning, has been demonstrated as a fascinating and effective technology for mass production of nanofibers [8-11]. The blown bubble-spinning can obtain hierarchically structured nanofibrous yarns by utilizing high temperature and high-speed airflow to directly blow and stretch polymer multi-bubbles [12-14]. The principle of this one step method is similar to that of two well-known technologies, melt-blowing and solution blowing [15, 16], which makes full use of air drawing force.

* Corresponding author, e-mail: hejihuan@suda.edu.cn

Moreover, the blown bubble spinning is mainly focused on overcoming the surface tension of a polymer bubble which geometrically depends upon its size and the pressure difference [17].

In this paper, effect of solution concentrations on the influence and controllability of blown bubble-spinning will be studied. In addition, the structure and properties will also be investigated to further explore the feasibility and scaling-up of this method.

Experimental

The Nylon6/66 ($C_{18}H_{37}N_3O_5$, Mw = 375.5 kDa) was purchased from Sigma, USA. The spun solutions were prepared by dissolving nylon6/66 at three different concentrations (9%, 12%, and 15%) in formic acid (88% v/v, Sinopharm Chemical Reagent Co., Ltd, China) under slight stirring for four hours.

As previously described by our group [18-20], compressed gas was released inside the solution to generate continuous bubbles at the orifice. Meanwhile, the blowing hot air in the form of two streams, that shaped a 60° angle, pulled the droplets of the bubble upwards rapidly and steadily, then nanofibers were obtained on the above collector. The diameter of orifice was 10 mm and the die to collector distance was 35 cm. This procedure was repeated by setting the air-flow temperature 160 ℃ and air-flow velocity 40 m/s.

Wilhelmy plate method was used for the surface tension tests on DTAC-21 Dynamic Contact Angle and Tension Tester at room temperature. Rheological tests of three spun solutions were run on a Rheometer (AR2000, TA Instruments, America) with a 40 mm cone plate (Ti, 40/2°). The normal force applied on the sample during lowering of the top plate was limited to 0.1 N. The shear rate was linearly increased from 0.01 to 5000 s^{-1} at 25 °C. The morphology of nanofibers was observed using an SEM (Hitachi S-4800, Japan) at 20 ℃, 60% RH. Samples were mounted on a copper plate and sputter-coated with gold layer 20-30 nm thick prior to imaging. The diameters of the products obtained were measured from randomly collected SEM images using the Image J software and expressed as mean ± standard deviation (SD). Thermogravimetric analysis (Q600, TA Instrument, America) were used to measure the thermal stability, and test conditions were nitrogen flow at 30 mL per minute, heating rate at 10 ℃ per minute, and temperature range from 50 °C to 600 ℃. The samples with a clamping length of 10 mm were placed at the standard conditions (20 ± 2 °C, RH 65 ± 5%) for 24 hours, and then measured on a mechanical testing instrument (Instron 3365, America) equipped with a 2cN load cell at a stretch speed of 10 mm per minute. The data reported were the average tensile properties from five specimens.

Results and discussion

Solution concentrations played a key role in the spinnability and resultant outcomes. As can be seen from fig. 1(a), with the increase of the concentration of PA6/66 (polyamide), the surface tension of solutions increased, which flattens out after 12%. Moreover, all surface tension of the three spinning solutions was greater than that of the solvent pure formic acid at 37.89 mN/m.

The viscosity characteristics of polymer have an important influence on its material forming and post-processing. It can be clearly seen from fig. 1(b) that with the increase of spinning concentrations at the same shear rate, the zero shear viscosity of the solution increased, which was consistent with many experimental and theoretical conclusions, as shown in the relation of subscale law:

$$\eta \propto C^{\alpha}$$

where η is the solution viscosity, C – the solution concentration, and α – the scaling law.

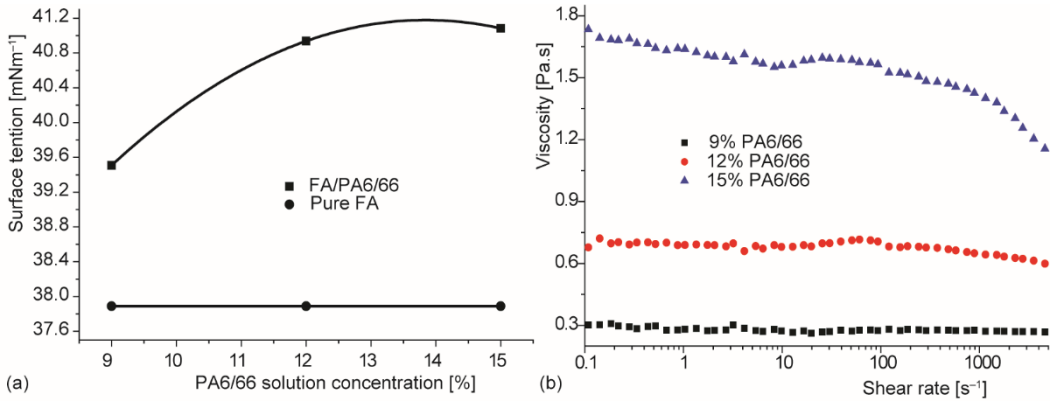

Figure 1. The relationship between solution concentrations and surface tension (a) and viscosity (b)

However, the viscosity of the solution varied slightly with the shear rate. In 9% spinning solution, the viscosity did not obviously change with the shear rate, showing the characteristics of Newtonian fluid. The properties of 12% spinning solution were the same as 9% spinning solution when the shear rate was less than 100 s^{-1}, but the viscosity gradually declined with a climb of the shear rate when the viscosity was greater than 100 s^{-1}. The 15% spinning solution showed significant shear thinning, which viscosity decreased with the increase of the shear rate. The main reason is that there are more physical crosslinks between polymer macromolecules when the solution concentration is high, and it is easier to get entangled with each other to increase the solution viscosity. With the increase of shear rate, the physical intersection points between macromolecular chains are destroyed, the orientation is increased, so the viscosity is decreased.

Figure 2 shows the SEM of PA6/66 nanofibers and yarns obtained by blown bubble--spinning under three different solution concentrations. As could be seen, the yarns contained a large number of beaded particles at 9% solution concentration, but nanofibers with a high degree of parallelization were very fine, about 300 nm. When the concentration increased to 12%, the beads disappeared and the yarns consisted of well-formed nanofibers were smooth and uniform. Besides, the diameter of yarns and nanofibers increased to 40.2 ±5.9 μm and 423.9 ±73.6 nm, respectively. When the solution concentration got to 15%, the diameter of the nanofibrous yarns became significantly coarser and the inside nanofibers with 754.4 ±172.6 nm diameter became looser. The reasons for the aforementioned phenomenon are mainly as follows: when the solution concentration is low, its viscosity is low as observed before, leading to weakly entangled molecular chains as well as slow solvent evaporation, so there will be spherical beads. On the other side, the surface tension of the solution with low concentration is also low, which needs weak resistance to be overcome during the airflow stretching, causing high nanofiber parallelization. As the solution concentration increases, the viscosity and surface tension of the solution also increase, resulting in higher drag force for external airflow to overcome and the occurrence of solution solidification into fibers in advance, which forms thicker nanofibers.

Figure 3 shows the DTA curve of PA6/66 nanofibrous yarns fabricated by blown bubble-spinning under different solution concentrations. According to fig. 3, the whole ther-

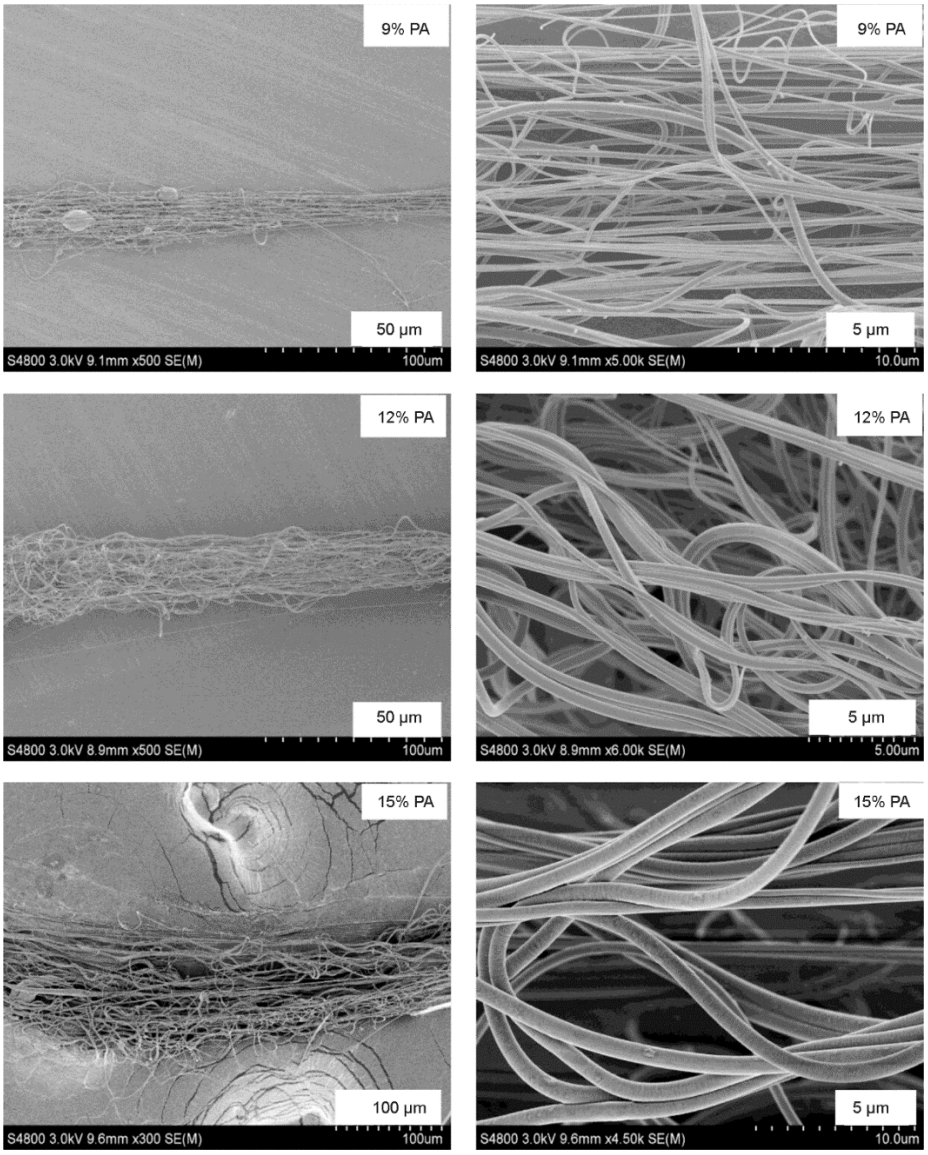

Figure 2. The SEM of PA6/66 nanofibers and yarns under different solution concentrations

mal decomposition process mainly had three endothermic processes: the first stage was below 100 ℃, which was ascribed to the evaporation of free water and combined water in samples. In the second stage, the yarns melt around 260 ℃, which needed to absorb heat to overcome the intermolecular forces. During the third stage around 420 ℃, the endothermic peak was mainly formed by the homolysis of molecular chains in the yarns as well as breaking amide bonds. Based on the comparison of melting temperature, T_m, and decomposition peak temperature, T_p, of different three nanofibrous yarns, it clearly indicated that both the melting temperature, T_m, and decomposition peak temperature, T_p, rose with the increase of spinning solution concentrations, which improved the thermal stability.

The mechanical property of yarns is one of yarns' important properties, which is closely related to its post-processing and subsequent applications. Figure 4 depicted the stress-strain curve of PA6/66 nanofibrous yarns spun by blown bubble-spinning under three concentration solutions. It was explicitly observed that with a growth of spinning liquid concentration, the breaking strength and initial modulus of the nanofibrous yarns gradually increased, while the breaking elongation first increased and then went down. The main reasons for this phenomenon are easy to recognize: the nanofibers obtained are very thin and soft at low spinning concentration, so their initial modulus is low but the elongation at break is high. However, due to liquid droplets in the yarns, which is similar to the *weak ring* in the uneven strip, the poor strength of single nanofiber leads to low quality of the nanofibrous yarns. With the spinning concentration improving, the resistance to external forces increases, resulting from an increase of the nanofibers. Nevertheless, owing to the thickening of nanofibers' diameter, the tightness between nanofibers drops so that the slip between nanofibers is easy to occur. Therefore, the tensile resistance is strong in the early stretching stage while the elongation at break decreases. In brief, nanofibrous yarns need post-treatments for enhancement of mechanical property.

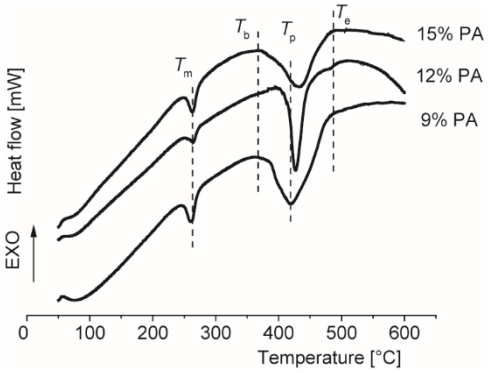

Figure 3. The thermal property of PA6/66 nanofibers and yarns under different solution concentrations; T_m – melting temperature, T_b – decomposition beginning temperature, T_p – decomposition peak temperature, T_e – decomposition ending temperature

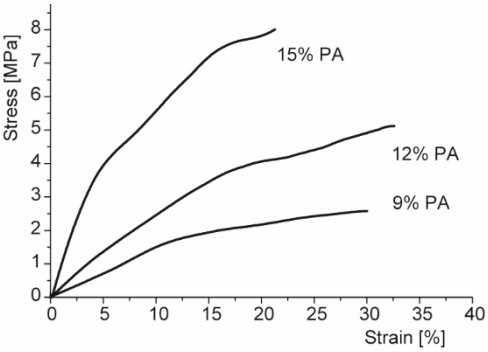

Figure 4. The stress-strain curve of PA6/66 nanofibers and yarns under different solution concentrations

Conclusion

Solution concentrations offer an effective way to control the structure of both nanofibers and nanofibrous yarns as well as to adjust the properties of final yarns obtained by the blown bubble-spinning, which is not affected by the Taylor cone as that in the traditional electrospinning [21]. For the further applications, solution properties and processing parameters should be optimized and post-treatments like hot stretching and annealing could be considered for high strength and high toughness, which will make contributions to the improvements of nanofibrous yarns fabricated by the blown bubble-spinning.

Acknowledgment

The work is supported by the Natural Science Basic Research Plan in Shaanxi Province of China (Program No. 2017JQ5054), the Doctoral Scientific Research Foundation of Xi'an Polytechnic University (BS15015), Thousand Talents Program of Shaanxi Province, San-qin Scholar Foundation of Shaanxi Province, National Natural Science Foundation of China (Grants No. 51802244 and No. 51603163) and Priority Academic Program Development of Jiangsu Higher Education Institutions (PAPD).

References

[1] Liao, X., *et al.*, High Strength in Combination with High Toughness in Robust and Sustainable Polymeric Materials, *Science, 366* (2019), 6471, pp. 1376-1379
[2] Li, X., *et al.*, Conjugate Electrospinning of Continuous Nanofiber Yarn of Poly (L-Lactide)/Nanotricalcium Phosphate Nanocomposite, *Journal of Applied Polymer Science, 107* (2008), 6, pp. 3756-3764
[3] Wang, X., *et al.*, Continuous Polymer Nanofiber Yarns Prepared by Self-Bundling Electrospinning Method, *Polymer, 49* (2008), 11, pp. 2755-2761
[4] Yousefzadeh, M., *et al.*, Producing Continuous Twisted Yarn from Well-Aligned Nanofibers by Water Vortex, *Polymer Engineering & Science, 51* (2011), 2, pp. 323-329
[5] Baniasadi, M., *et al.*, High-Performance Coils and Yarns of Polymeric Piezoelectric Nanofibers, ACS *Applied Materials & Interfaces, 7* (2015), 9, pp. 5358-5366
[6] Yang, E., *et al.*, Influence of Electric Field Interference on Double Nozzles Electrospinning, *Journal of Applied Polymer Science, 116* (2010), 6, pp. 3688-3692
[7] Walmsley, H. L., Electrostatic Ignition Hazards with Plastic Pipes at Petrol Stations, *Journal of Loss Prevention in the Process Industries, 25* (2012), 2, pp. 263-273
[8] Li, X. X., *et al.*, Bubble Electrospinning with an Auxiliary Electrode and an Auxiliary Air Flow, *Recent Patents on Nanotechnology, 14* (2020), 1, pp. 42-45
[9] Yin, J., *et al.* Numerical Approach to High-Throughput of Nanofibers by a Modified Bubble-Electrospinning, *Thermal Science, 24* (2020), 4, pp. 2367-2375
[10] He, J.-H., Liu, Y. P., Bubble Electrospinning: Patents, Promises and Challenges, *Recent Patents on Nanotechnology, 14* (2020), 1, pp. 3-4
[11] He, J.-H., Advances in Bubble Electrospinning, *Recent Patents on Nanotechnology, 13* (2019), 3, pp. 162-163
[12] He, J.-H., *et al.*, Review on Fiber Morphology Obtained by Bubble Electrospinning and Blown Bubble Spinning, *Thermal science, 16* (2012), 5, pp. 1263-1279
[13] Dou, H., *et al.*, Blown Bubble-Spinning for Fabrication of Superfine Fibers, *Thermal Science, 16* (2012), 5, pp. 1465-1466
[14] Liu, H. Y., *et al.*, A Novel Method for Fabrication of Fascinated Nanofiber Yarns, *Thermal Science, 19* (2015), 4, pp. 1331-1335
[15] Chen, T., *et al.*, Numerical Computation of the Fiber Diameter of Melt Blown Nonwovens Produced by the Inset Die, *Journal of applied polymer science, 111* (2009), 4, pp. 1775-1779
[16] Borkar, S., *et al.*, Polytetrafluoroethylene Nano/Microfibers by Jet Blowing, *Polymer, 47* (2006), 25, pp. 8337-8343
[17] He, J.-H., Effect on Temperature on Surface Tension of a Bubble and Hierarchical Ruptured Bubbles for Nanofiber Fabrication, *Thermal Science, 16* (2012), 1, pp. 327-330
[18] Dou, H., *et al.*, Effect of MWCNT on the Structure and Property of Nanofibrous Bundles by The Blown Bubble Spinning, *Recent Patents on Current Nanotechnology, 13* (2019), 3, pp. 171-180
[19] Dou, H., *et al.*, Effect of Air-Flow Parameters on the Morphology of Nanofibrous Yarns by Blown Bubble-Spinning, *Thermal Science, 24* (2020), 4, pp. 2637-2643
[20] Liu, H. Y., Fascinated Nanofiber Yarns: From Experiment to Industrialization, *Recent Patents on Current Nanotechnology, 14* (2020), 1, pp.71-74
[21] He, J.-H., On the Height of Taylor Cone in Electrospinning, *Results in Physics, 17* (2020), June, ID 103096

Paper submitted: March 1, 2020
Paper revised: July 13, 2020
Paper accepted: July 13, 2020